EMBO reports

scientific report

Upstream promoter sequences and αCTD mediate stable DNA wrapping within the RNA polymerase–promoter open complex

Sara Cellai[1], Laura Mangiarotti[1], Nicola Vannini[1], Nikolai Naryshkin[2†], Ekaterine Kortkhonjia[2‡], Richard H. Ebright[2+] & Claudio Rivetti[1++]

[1]Department of Biochemistry and Molecular Biology, University of Parma, Parma, Italy, [2]Department of Chemistry, Waksman Institute, and Howard Hughes Medical Institute, Rutgers University, Piscataway, New Jersey, USA

We show that the extent of stable DNA wrapping by *Escherichia coli* RNA polymerase (RNAP) in the RNAP–promoter open complex depends on the sequence of the promoter and, in particular, on the sequence of the upstream region of the promoter. We further show that the extent of stable DNA wrapping depends on the presence of the RNAP α-subunit carboxy-terminal domain and on the presence and length of the RNAP α-subunit interdomain linker. Our results indicate that the extensive stable DNA wrapping observed previously in the RNAP–promoter open complex at the λ P_R promoter is not a general feature of RNAP–promoter open complexes.

Keywords: α carboxy-terminal domain; atomic force microscopy; DNA wrapping; transcription; UP elements

EMBO reports (2007) **8**, 271–278. doi:10.1038/sj.embor.7400888

INTRODUCTION

Atomic force microscopy (AFM) allows straightforward detection and quantification of DNA compaction by DNA-binding proteins (Rivetti *et al*, 1999; Verhoeven *et al*, 2001; Heddle *et al*, 2004). DNA compaction is observed as a reduction of the DNA contour length in the presence of the DNA-binding protein of interest with respect to free DNA.

In previous work, using AFM, it has been shown that *Escherichia coli* RNA polymerase (RNAP) results in massive, ~30 nm, apparent DNA compaction on formation of a catalytically competent RNAP–promoter open complex (RP_o) at the λ P_R promoter (Rivetti *et al*, 1999). On the basis of the dimensions of RNAP (~10 nm × ~10 nm × ~15 nm; Zhang, 1999), the structure of RNAP (Zhang, 1999), and the modelled structure of RP_o (Naryshkin *et al*, 2000), this massive apparent DNA compaction must arise from wrapping or spooling of upstream promoter DNA (promoter positions −100 to −40) around RNAP (Naryshkin *et al*, 2000). To account for the full extent of the apparent DNA compaction in RP_o at the λ P_R promoter, it is necessary to invoke wrapping of upstream promoter DNA by nearly 300° around RNAP (Coulombe & Burton, 1999; Rivetti *et al*, 1999). Interactions between upstream promoter DNA and RNAP, presumably dependent on at least partial wrapping of upstream promoter DNA around RNAP, have been shown to affect the rate of formation of RP_o (Davis *et al*, 2005; Ross & Gourse, 2005) and have been proposed to affect the rate of entry of DNA into, and unwinding of DNA in, the RNAP active centre cleft (Davis *et al*, 2005).

In this work, using AFM, we assess the effects of the promoter sequence, the RNAP α-subunit carboxy-terminal domain (αCTD) and the RNAP α-subunit interdomain linker (α-linker) on DNA compaction by RNAP. We find that DNA compaction depends on the sequence of the upstream region of the promoter, the presence of αCTD and the presence and length of the α-linker. Our results indicate that the sequence of the upstream region of the promoter affects DNA compaction not only through effects on αCTD–DNA interaction but also through other effects—presumably effects on intrinsic DNA curvature. Our results further indicate that, in the absence of αCTD–DNA interaction with upstream promoter DNA and intrinsic DNA curvature in the upstream region of the promoter, DNA compaction by RNAP is only ~2–4 nm, consistent with the expectation from the modelled structure of RP_o (Naryshkin *et al*, 2000). Overall, our results indicate that the massive, ~30 nm, DNA compaction observed previously in RP_o at the λ P_R promoter (Rivetti *et al*, 1999) is not a general feature of RP_o at all promoters.

[1]Department of Biochemistry and Molecular Biology, University of Parma, Viale G.P. Usberti 23/A, 43100 Parma, Italy
[2]Department of Chemistry, Waksman Institute, 190 Frelinghuysen Road, Piscataway, New Jersey 08854, USA
[†]Present address: PTC Therapeutics, 100 Corporate Court, South Plainfield, New Jersey 07080, USA
[‡]Present address: Department of Chemistry and Biochemistry, University of California at Los Angeles (UCLA), 607 Charles E. Young Drive East, Los Angeles, California 90095, USA
[+]Corresponding author. Tel: +1 732 445 5179; Fax: +1 732 445 5312; E-mail: ebright@mbcl.rutgers.edu
[++]Corresponding author. Tel: +39 0521 905649; Fax: +39 0521 905151; E-mail: claudio.rivetti@unipr.it

Received 26 May 2006; revised 2 November 2006; accepted 23 November 2006; published online 9 February 2007

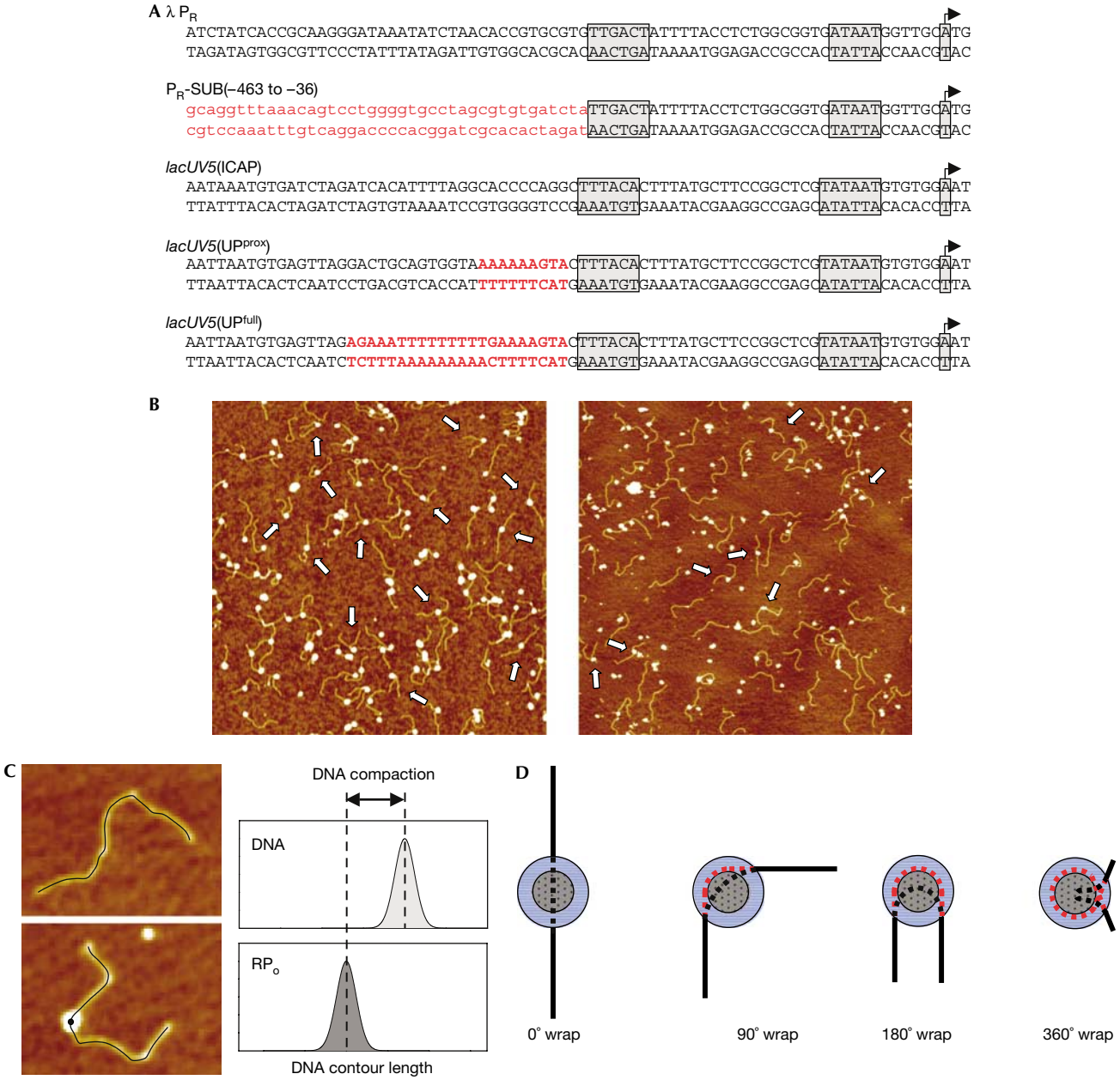

Fig 1 | Atomic force microscopy measurements of DNA compaction. (**A**) Promoters analysed in this work. In each sequence, the transcription start site, the −10 and −35 hexamers are boxed. In P_R-SUB(−463 to −36), heterologous DNA is shown in red, lower case; in *lacUV5*(UP^{prox}), the consensus proximal UP-element subsite (Estrem *et al*, 1999) is shown in red; in *lacUV5*(UP^{full}), the consensus full UP element (Estrem *et al*, 1998) is shown in red. (**B**) Representative atomic force microscopy images of RP_o formed with wild-type RNAP at the λ P_R promoter (left) or the *lacUV5*(ICAP) promoter (right). Arrows point to individual complexes. The image scan size is 2 μm. (**C**) Measurement of apparent DNA contour lengths in the absence (top) and presence (bottom) of RNAP. (**D**) Relationship between apparent DNA compaction and stable DNA wrapping. Grey dotted circle, RNAP; blue circle, tip broadening effect; black line, protein-free DNA; red dashed line, hidden DNA path; black dashed line, inferred DNA path through the centre of the RNAP. Apparent DNA compaction equals the difference in length between the red dashed line and the black dashed line. RNAP, RNA polymerase; RP_o, RNA polymerase–promoter open complex.

RESULTS

AFM measurements of DNA compaction in RP_o

In this work, RNAP and RNAP derivatives were used to prepare RP_o at the λP_R and *lacUV5* promoters, or at substituted derivatives of these promoters (Fig 1A). Complexes were deposited onto freshly cleaved mica and imaged in air by AFM, and DNA contour lengths were measured (Fig 1B). Protein-induced apparent DNA compaction is defined as the difference between (i) the DNA contour length in the absence of protein (Fig 1C, top) and (ii) the DNA contour length of RNAP–DNA complexes (Fig 1C, bottom).

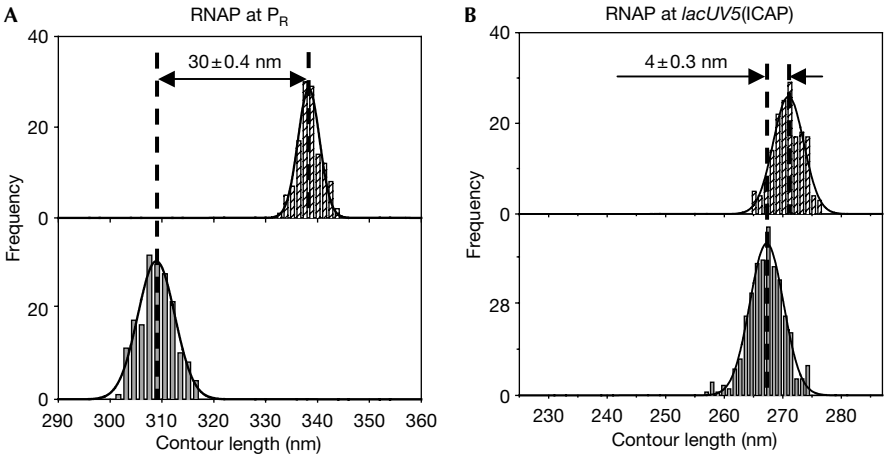

Fig 2 | The extent of DNA compaction depends on the sequence of the promoter. (**A**,**B**) Contour length distributions of DNA in the absence (hatched bars; top) and presence (grey bars; bottom) of RNAP are shown. Apparent DNA compaction is presented as mean±s.e.m. RNAP, RNA polymerase.

This compaction was used as a quantitative indicator of protein-induced stable DNA wrapping, with a large compaction interpreted as a large protein-induced stable DNA wrapping (Fig 1D; Rivetti *et al*, 1999; Verhoeven *et al*, 2001; Heddle *et al*, 2004). Free contour length measurements were made by tracing the DNA path from end to end, as described previously (Rivetti & Codeluppi, 2001). The contour length of RNAP–DNA complexes was measured by tracing the DNA path from end to end and passing through the centre of the protein (Rivetti *et al*, 1999). In the case of protein–DNA complexes, the measurements are complicated because DNA in contact, or in close proximity, with the protein potentially can be hidden by tip-broadening and out-of-plane effects (Bustamante, 1993; Bustamante & Rivetti, 1996). This might result in underestimation of protein-free DNA contour lengths and overestimation of apparent DNA compaction. In the case of a large protein, such as RNAP, this effect can be up to ~5 nm. Accordingly, in this work, an apparent DNA compaction is deemed significant as an indicator of stable DNA wrapping only if it is >5 nm.

Surface interactions on deposition onto mica can also potentially cause an artefactual apparent DNA compaction (Rivetti *et al*, 1996). Accordingly, in this work, we used deposition conditions that allow complete configurational equilibration of DNA (Rivetti *et al*, 1996) as confirmed by the observation that mean-square end-to-end distances of DNA in the absence of RNAP were in the range predicted for an ideal worm-like chain polymer at equilibrium in two dimensions (data not shown; see Rivetti *et al*, 1996). It is thus believed that, under the conditions used, complexes were not significantly distorted by the deposition process (Bustamante & Rivetti, 1996).

DNA compaction depends on promoter sequence

Figure 2 and Table 1 present data for RNAP–promoter complexes at the λ P_R and *lacUV5*(ICAP) promoters. For λ P_R, an apparent DNA compaction of 30±0.4 nm was observed, consistent with previous results (Rivetti *et al*, 1999). By contrast, for *lacUV5*(ICAP), a strikingly smaller apparent DNA compaction, only 4±0.3 nm, was observed. Control experiments established that in the presence of nucleotides, 69% of the complexes formed at λ P_R and 70% of the complexes formed at *lacUV5*(ICAP) can actively transcribe the downstream DNA. This indicates that most of the promoter-bound complexes were active RP_o (supplementary Table S1 and Fig S1 online). We conclude that the extent of apparent DNA compaction in RP_o is not constant from promoter to promoter, but, instead, depends on promoter sequence.

DNA compaction depends on upstream elements

To determine whether DNA compaction depends on sequence determinants in the upstream region of the promoter, we assessed DNA compaction in RNAP–promoter complexes at P_R-SUB(−463 to −36), a P_R derivative having a substitution replacing all sequences between positions −463 and −36 (Fig 1A). A large DNA compaction of 30±0.4 nm was observed for P_R, whereas a strikingly smaller DNA compaction, of only 6±0.8 nm, was observed for P_R-SUB(−463 to −36; Fig 3A; Table 1). Control experiments established that, in the presence of nucleotides, 77% of the complexes formed at P_R-SUB(−463 to −36) were active RP_o (supplementary Table S1 and Fig S1 online). We conclude that DNA compaction in RP_o depends on sequence determinants in the upstream region of the promoter.

Two classes of upstream region promoter elements have been defined: the UP-element subsite and the full UP element (Estrem *et al*, 1998, 1999; Gourse *et al*, 2000). The UP-element subsite (a short A/T-rich sequence centred in the −93, −83, −73, −63, −53 or, optimally, −43 region) stimulates transcription up to ~200-fold through interactions with one RNAP αCTD (Estrem *et al*, 1999; Gourse *et al*, 2000). The full UP element (two adjacent UP-element subsites, optimally one centred in the −53 region and the other centred in the −43 region) stimulates transcription up to ~300-fold through interactions with two RNA αCTDs (Estrem *et al*, 1998; Gourse *et al*, 2000).

To determine whether DNA compaction can be affected by a UP-element subsite or a full UP element, we assessed DNA compaction in RNAP–promoter complexes at the *lacUV5*(UP^{prox}) and *lacUV5*(UP^{full}) promoters, respectively, a *lacUV5* derivative containing a consensus UP-element subsite centred in the −43 region and a *lacUV5* derivative containing a consensus full UP element centred in the −53/−43 region (Fig 1A; Estrem *et al*,

Table 1 | DNA compaction in RP_o

RNAP	Promoter	DNA length (bp)	Bare DNA contour length (nm)	DNA contour length of RP_o (nm)	DNA compaction (nm)
RNAP	λ P_R	1,054	338 ± 0.2 (N = 126)	308 ± 0.3 (N = 177)	30 ± 0.4
RNAP	P_R-SUB(−463 to −36)	963	317 ± 0.6 (N = 112)	311 ± 0.5 (N = 168)	6 ± 0.8
RNAP	*lacUV5*(ICAP)	832	271 ± 0.2 (N = 166)	267 ± 0.2 (N = 354)	4 ± 0.3
RNAP	*lacUV5*(UP^{prox})	1,050	347 ± 0.3 (N = 109)	345 ± 0.4 (N = 130)	2 ± 0.5
RNAP	*lacUV5*(UP^{full})	1,191	378 ± 0.3 (N = 101)	357 ± 0.6 (N = 130)	21 ± 0.7
$\Delta\alpha CTD^{I}$ /$\Delta\alpha CTD^{II}$ RNAP	λ P_R	1,054	344 ± 0.3 (N = 76)	334 ± 0.6 (*) (N = 130)	10 ± 0.7
$\Delta\alpha CTD^{I}$ /$\Delta\alpha CTD^{II}$ RNAP	*lacUV5*(ICAP)	832	269 ± 0.5 (N = 83)	265 ± 0.7 (N = 73)	4 ± 0.8
$\Delta\alpha CTD^{I}$ /$\Delta\alpha CTD^{II}$ RNAP	*lacUV5*(UP^{full})	1,050	343 ± 0.3 (N = 91)	330 ± 0.5 (N = 79)	13 ± 0.6
$\Delta\alpha CTD^{II}$ RNAP	λ P_R	1,054	348 ± 0.3 (N = 141)	335 ± 0.2 (N = 466)	13 ± 0.4
$\Delta\alpha CTD^{II}$ RNAP	*lacUV5*(ICAP)	832	266 ± 0.7 (N = 93)	261 ± 2.5 (§) (N = 41)	5 ± 2.0
$\Delta\alpha CTD^{II}$ RNAP	*lacUV5*(UP^{full})	1,050	345 ± 0.3 (N = 92)	332 ± 0.5 (N = 55)	13 ± 0.5
$\Delta 6\text{-}\alpha^{I}/\Delta 6\text{-}\alpha^{II}$ RNAP	λ P_R	1,054	349 ± 0.3 (N = 203)	334 ± 0.4 (*) (N = 182)	15 ± 0.4
$\Delta 6\text{-}\alpha^{I}/\Delta 6\text{-}\alpha^{II}$ RNAP	*lacUV5*(UP^{full})	1,050	345 ± 0.3 (N = 81)	332 ± 0.6 (N = 51)	13 ± 0.6
$\Delta 12\text{-}\alpha^{I}/\Delta 12\text{-}\alpha^{II}$ RNAP	λ P_R	1,054	349 ± 0.3 (N = 121)	335 ± 0.6 (*) (N = 122)	14 ± 0.6
$\Delta 12\text{-}\alpha^{I}/\Delta 12\text{-}\alpha^{II}$ RNAP	*lacUV5*(UP^{full})	1,050	341 ± 0.5 (N = 40)	329 ± 1.0 (N = 35)	12 ± 1.1

Contour length values of DNA in the absence of RNAP and RP_o represent the mean ± standard error of the mean (s.e.m.) obtained from the fitting of the DNA contour length distributions shown in Figs 2–5. In the case of bimodal distributions (*), values refer to the leftmost peak. (§) Because of the paucity and scatter of the data, this value represents the arithmetical average of the distribution. The basis for the no-compaction peak observed in Figs 3D,5A,B is not known, but might represent a subpopulation of RNAP–promoter closed complexes that exhibit no compaction (supplementary Fig S2 online; Rippe *et al*, 1997). *N* represents the number of molecules measured for each data set. The DNA compaction is given by the difference between the DNA contour length of DNA in the absence of RNAP and that of RP_o.

1998, 1999). A DNA compaction of only 2 ± 0.5 nm was observed for the *lacUV5*(UP^{prox}) promoter (Fig 3B; Table 1), whereas a DNA compaction of 21 ± 0.7 nm was observed for *lacUV5*(UP^{full}) promoter (Fig 3C; Table 1). Control experiments established that, in the presence of nucleotides, 76% of the complexes formed at *lacUV5*(UP^{full}) were active RP_o (supplementary Table S1 and Fig S1 online). We again conclude that DNA compaction in RP_o depends strongly on sequence determinants in the upstream region of the promoter. We further conclude that a full UP element, but not a single UP-element subsite (at least not a single proximal UP-element subsite), represents a sequence determinant for large DNA compaction in RP_o.

DNA compaction depends on the presence of the αCTD

RNAP (subunit composition $\beta'\beta\alpha^{I}\alpha^{II}\omega\sigma^{70}$) contains two identical α-subunits, α^{I} and α^{II}. Each α-subunit consists of (i) an amino-terminal domain (αNTD) with determinants for dimerization and for interaction with β′ and β, (ii) an αCTD with determinants for protein–DNA interaction with UP-element subsites and for protein–protein interactions with transcriptional regulators and (iii) a long, flexible interdomain linker (α-linker; Blatter *et al*, 1994; Busby & Ebright, 1994). The long, flexible α-linker allows αCTD to occupy different positions relative to αNTD—and thus relative to the remainder of RNAP—in different RNAP–promoter complexes (i.e. to interact nonspecifically with upstream DNA at a simple promoter, to interact with a UP-element subsite or UP element at a UP-element-subsite- or UP-element-containing promoter or to interact with an activator at an activator-dependent promoter; Busby & Ebright, 1994).

To determine whether DNA compaction is dependent on the presence of αCTD, we assessed DNA compaction in RP_o prepared using $\Delta\alpha CTD^{I}/\Delta\alpha CTD^{II}$ RNAP, an RNAP derivative lacking both αCTD^{I} and αCTD^{II}, at the λ P_R and *lacUV5*(UP^{full}) promoters. At P_R, a DNA compaction of 30 ± 0.4 nm was observed with wild-type (WT)-RNAP, but a significantly smaller DNA compaction, of only 10 ± 0.7 nm, was observed with $\Delta\alpha CTD^{I}/\Delta\alpha CTD^{II}$ RNAP (Fig 3D; Table 1). Similarly, at *lacUV5*(UP^{full}), a DNA compaction of 21 ± 0.7 nm was observed with WT-RNAP, but a significantly smaller DNA compaction, of only 13 ± 0.6 nm, was observed with $\Delta\alpha CTD^{I}/\Delta\alpha CTD^{II}$ RNAP (Fig 3E; Table 1). As expected, a DNA compaction of 4 ± 0.8 nm was observed with $\Delta\alpha CTD^{I}/\Delta\alpha CTD^{II}$ RNAP at *lacUV5*(ICAP) (Fig 3F; Table 1). We conclude that the extent of DNA compaction depends on the presence of αCTD.

To determine whether DNA compaction is dependent on the presence of both αCTD^{I} and αCTD^{II}, we assessed DNA compaction in RP_o assembled with $\Delta\alpha CTD^{II}$ RNAP, an RNAP derivative having αCTD^{I} but lacking αCTD^{II} (Estrem *et al*, 1999) at the λ P_R and *lacUV5*(UP^{full}) promoters. At P_R, only a small DNA compaction, of 13 ± 0.4 nm, was observed with $\Delta\alpha CTD^{II}$ RNAP (a DNA compaction comparable with that observed with $\Delta\alpha CTD^{I}/\Delta\alpha CTD^{II}$ RNAP; Fig 4A; Table 1). Similarly, at *lacUV5*(UP^{full}), only a small DNA compaction, of 13 ± 0.5 nm, was observed with $\Delta\alpha CTD^{II}$ RNAP (Fig 4B; Table 1). As expected, a DNA compaction of 5 ± 2.0 nm was observed with $\Delta\alpha CTD^{II}$ RNAP at *lacUV5*(ICAP) (Fig 4C; Table 1). We conclude that αCTD^{I} alone is insufficient to mediate large-scale DNA compaction.

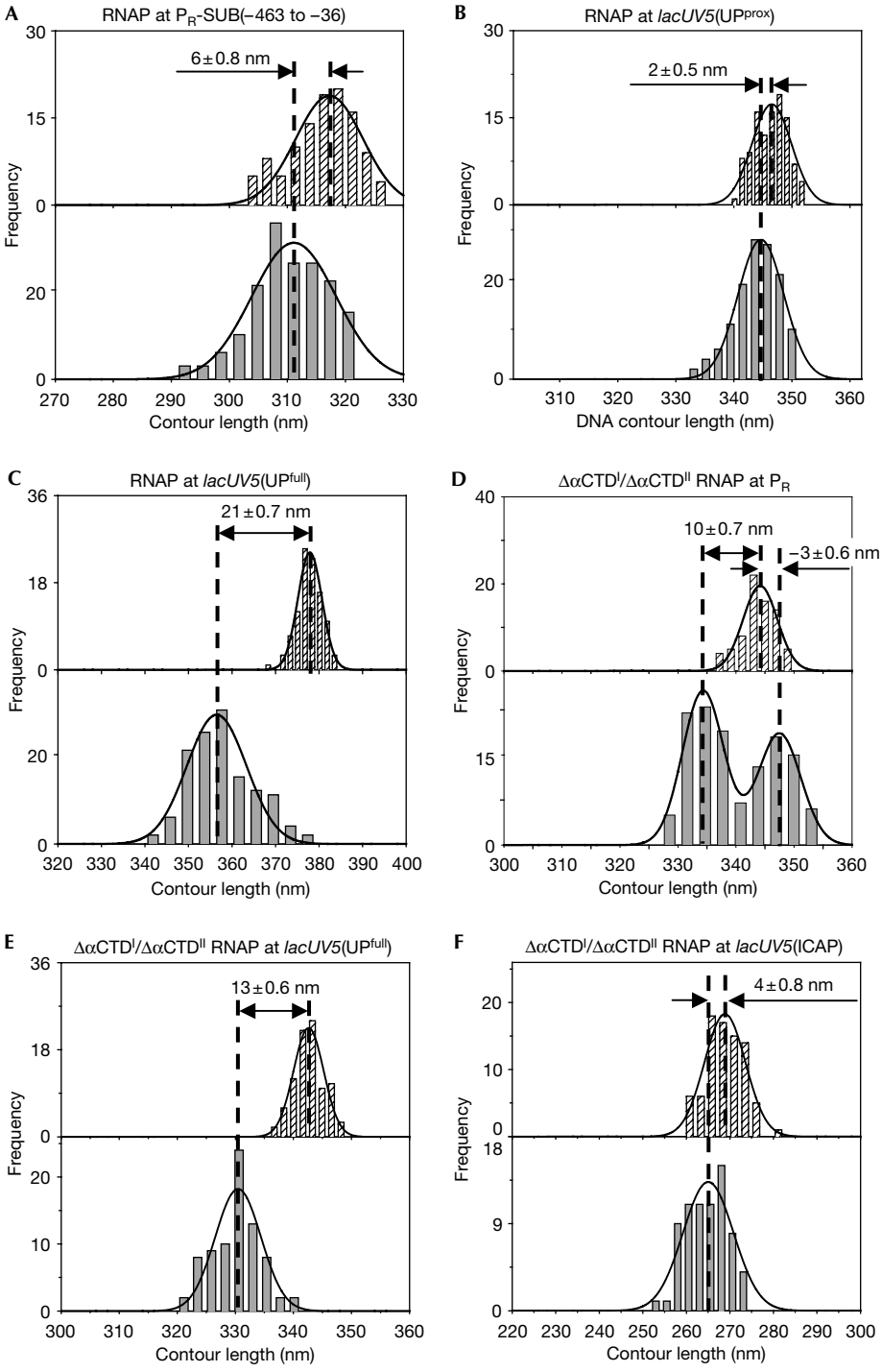

Fig 3 | The extent of DNA compaction depends on sequence determinants in the upstream region of the promoter and on αCTD. Contour length distributions of DNA in the absence (hatched bars; top) and presence (grey bars; bottom) of RNAP, from experiments with promoter derivatives having substituted upstream regions (**A–C**) and with RNAP derivatives lacking both αCTDs (**D–F**). Apparent DNA compaction is presented as mean ± s.e.m. αCTD, α-subunit carboxy-terminal domain; RNAP, RNA polymerase.

DNA compaction depends on the α-linker

The α-linker is ~15 amino acids in length and comprises α-residues from residue ~236 to ~251 (Blatter *et al*, 1994; Meng *et al*, 2000).

To determine whether DNA compaction is dependent on the presence and length of the α-linker, we assessed DNA compaction in RP_o assembled with Δ6-α^{I}/Δ6-α^{II} RNAP, an RNAP derivative lacking six amino-acid residues of the α-linker (α-residues

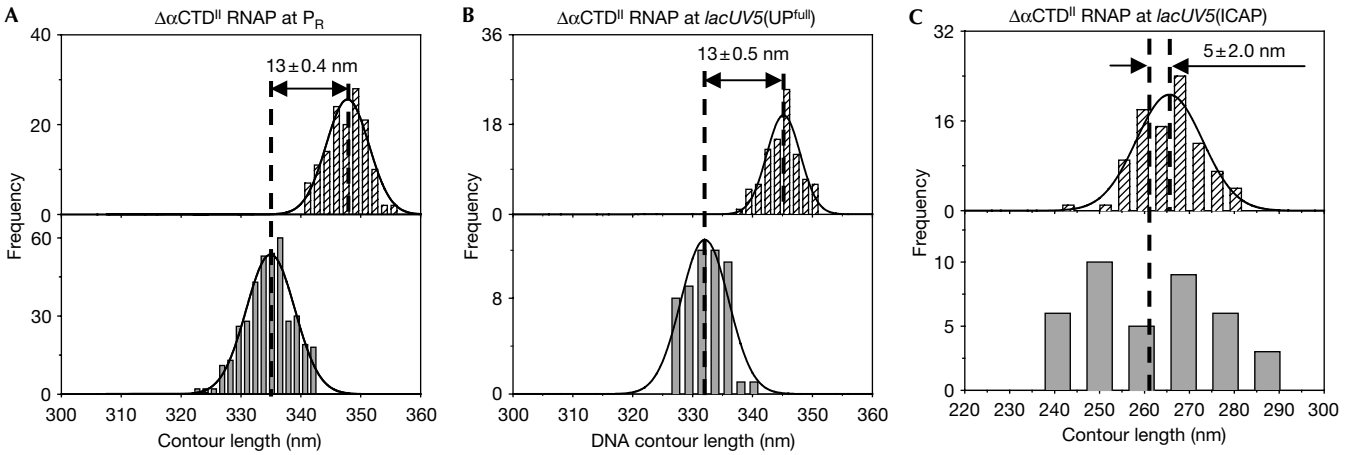

Fig 4 | αCTD^{I} alone is insufficient to mediate large-scale DNA compaction. (**A–C**) Contour length distributions of DNA in the absence (hatched bars; top) and presence (grey bars; bottom) of RNAP, from experiments with ΔαCTD^{II} RNAP derivatives. Apparent DNA compaction is presented as mean ± s.e.m. Because of the paucity and scatter of the data, the mean value in (**C**) represents the arithmetical average of the data. αCTD, α-subunit carboxy-terminal domain; RNAP, RNA polymerase.

235–241; Meng *et al*, 2000), and with Δ12-α^{I}/Δ12-α^{II} RNAP, an RNAP derivative lacking 12 amino-acid residues of the α-linker (α-residues 235–247; Meng *et al*, 2000).

At P_R, only a small DNA compaction, of 15 ± 0.4 or 14 ± 0.6 nm, was observed with Δ6-α^{I}/Δ6-α^{II} RNAP or Δ12-α^{I}/Δ12-α^{II} RNAP (a DNA compaction comparable with that observed with ΔαCTD^{I}/ΔαCTD^{II} RNAP; Fig 5A,B; Table 1). Similarly, at *lacUV5*(UP^{full}), only a small DNA compaction, of 13 ± 0.6 or 12 ± 1.1 nm, was observed with Δ6-α^{I}/Δ6-α^{II} RNAP and Δ12-α^{I}/Δ12-α^{II} RNAP (a DNA compaction comparable with that observed with ΔαCTD^{I}/ΔαCTD^{II} RNAP; Fig 5C,D; Table 1). We conclude that the α-linker is required for large-scale DNA compaction.

The DNA bend angle is coupled to the DNA compaction

The DNA bend angle, defined as the deviation from linearity of the double helix, was measured for each complex by means of tangents drawn at the exit points of DNA from RNAP. The data are shown in supplementary Figs S3–S6 online. Overall, there is a good correlation between DNA compaction and bend angle. For example, the DNA bend angle of WT-RNAP at P_R is 55 ± 2.4°, which is consistent with an almost complete turn of the DNA around the RNAP at this promoter (see also figure 8 in Rivetti *et al*, 1999). Conversely, at *lacUV5*(ICAP), the measured DNA bend angle is 16 ± 3.3°, which is consistent with the little DNA compaction observed at this promoter. At P_R-SUB(−463 to −36) and *lacUV5*(UP^{prox}) promoters, the DNA bend angles are 0 ± 4.8° and 18 ± 4.7°, respectively. These values correlate well with the little DNA compaction observed with these promoters. At *lacUV5*(UP^{full}), the measured DNA bend angle is 49 ± 1.4°, which is again consistent with the 21 nm DNA compaction observed at this promoter. Thus, we conclude that a large DNA compaction associated with a high DNA bend angle is the result of DNA wrapping around the RNAP.

A statistically significant correlation between DNA compaction and DNA bend angle cannot be attributed for complexes assembled with αCTD-RNAP mutants. This might be due to the intermediate DNA compaction observed in some of these cases, the presence of different types of complex as shown by the bimodal DNA contour length distributions and difficulties of obtaining narrow bend angle distributions.

DISCUSSION

Our results establish that the extent of stable DNA wrapping in RP_o depends on the sequence of the promoter and, in particular, on sequence determinants in the upstream region of the promoter (UP elements). The presence of αCTD and an intact α-linker is required to maintain extensive stable DNA wrapping. Our results further indicate that the sequence of the upstream region of the promoter can affect DNA wrapping even in the absence of αCTD and thus even in the absence of αCTD–DNA interactions. For example, RP_o prepared using ΔαCTD^{I}/ΔαCTD^{II} RNAP shows an apparent DNA compaction of 13 ± 0.6 nm at *lacUV5*(UP^{full}) but only 4 ± 0.8 nm at *lacUV5*(ICAP) (Fig 3E,F). We infer that the sequence of the upstream region of the promoter can affect compaction not only through effects on αCTD–DNA interaction but also through other effects. We suggest that these other effects involve intrinsic DNA curvature, noting that UP-element subsites and UP elements are A/T-rich sequences (Fig 1A; Ross *et al*, 1993) and that A/T-rich sequences are associated with intrinsic DNA curvature (Koo *et al*, 1986). In the absence of αCTD–DNA interaction with upstream promoter DNA and of intrinsic DNA curvature in upstream DNA, stable DNA wrapping in RP_o is small.

Overall, we show that tight, stable DNA wrapping is not a general feature of RP_o, but rather depends on the promoter sequence. The tight, stable DNA wrapping observed at λ P_R implies the presence, in the upstream region of this promoter, of sequence determinants that promote stable DNA wrapping—sequence determinants that, similar to the UP element in *lacUV5*(UP^{full}), make specific protein–DNA interactions with RNAP, favour intrinsic DNA curvature or both. A detailed analysis

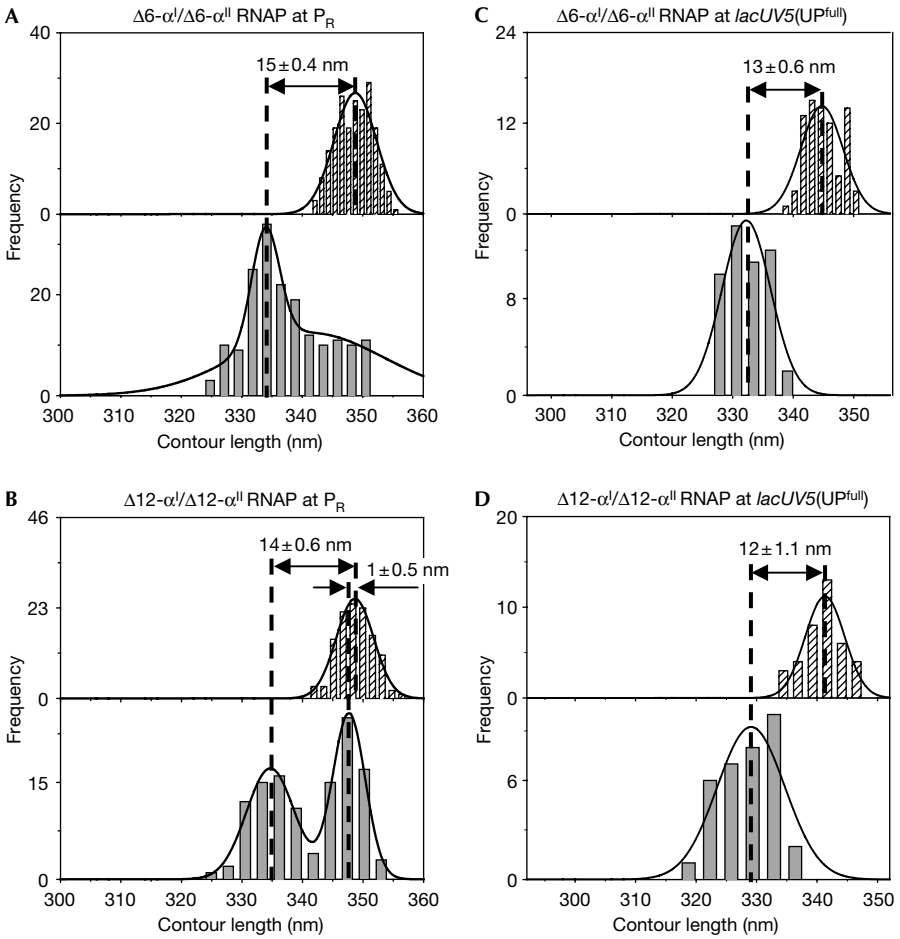

Fig 5 | The extent of DNA compaction depends on the length of the α-linker. (**A–D**) Contour length distributions of DNA in the absence (hatched bars; top) and presence (grey bars; bottom) of RNAP derivatives, from experiments with RNAP derivatives lacking residues of the α-linker. Apparent DNA compaction is presented as mean ± s.e.m. α-linker, α-subunit interdomain linker; RNAP, RNA polymerase.

of the sequence determinants responsible for stable DNA wrapping at λ P_R will be presented elsewhere.

Interestingly, as described in the supplementary information online, inactive promoter complexes (complexes in which RNAP is bound to the promoter but is unable to initiate RNA synthesis), in particular those formed at P_R and *lacUV5*(UP^{full}), have a mean DNA compaction that is significantly smaller than that of the corresponding active RP_o (supplementary Fig S2 and Table S2 online).

The results of photocrosslinking studies indicate that the αCTDs can interact sequence-nonspecifically with the upstream region of the *lacUV5* promoter, making sequence-nonspecific interactions with the DNA minor groove near positions −43, −53, −63, −73, −83 and −93 (Naryshkin *et al*, 2000). The results of promoter-truncation experiments indicate that the upstream region of the *lacUV5* promoter can influence the association of RNAP (Ross & Gourse, 2005). How can this evidence for upstream interactions at *lacUV5* be reconciled with the observed near-absence of apparent DNA compaction and thus the near-absence of stable DNA wrapping at *lacUV5*? We suggest that αCTD interacts only transiently with the upstream region of *lacUV5*, making interactions sufficient to allow crosslinking and to allow effects on the association of RNAP, but not sufficient to yield measurable DNA compaction at equilibrium (as in imaging by AFM under the conditions used in this work; see the discussion in the first section of Results; see also Bustamante & Rivetti, 1996). In this regard, we note that (i) the photogenerated reactive species used in photocrosslinking studies is relatively long-lived, allowing efficient sampling of transient interactions (Naryshkin *et al*, 2000; N.N. & R.H.E., unpublished data), and (ii) rapid quenching of the photogenerated reactive species eliminates crosslinking of αCTD with the upstream region of *lacUV5* (N.N. & R.H.E., unpublished data). Thus, results from photocrosslinking expressly support the occurrence of transient, as opposed to stable, interactions of αCTD with the upstream region of *lacUV5*.

An extended RNAP–DNA interaction can affect transcription in several, not mutually exclusive ways. A larger number of contacts between the RNAP and promoter DNA can increase the overall affinity of RNAP for the promoter (Aiyar *et al*, 1998; Estrem *et al*, 1998, 1999; Ross *et al*, 1993, 1998). An extended RNAP–DNA interaction, and corresponding DNA wrapping and wrapping-dependent distortion, also potentially can mechanically influence the isomerization from RNAP–promoter closed to RNAP–promoter open complex (Coulombe & Burton, 1999; Davis *et al*, 2005; Ross

& Gourse, 2005). However, it should be emphasized that, as shown in this work, tight, stable DNA wrapping is not a general feature of all RP_o at all promoters, but rather is strongly dependent on the promoter sequence.

METHODS

DNA templates and proteins. The 1,054-bp-long DNA fragment carrying λ P_R contains λ-DNA from –438 to +34 with respect to the P_R start site, which is positioned 616 bp from the downstream end. The 963-bp-long DNA fragment P_R-SUB(−463 to −36) contains λ-DNA from −35 to +34 with respect to the P_R start site, which is positioned 500 bp from the downstream end. The 832-bp-long DNA fragment carrying *lacUV5*(ICAP) has the start site positioned 360 bp from the downstream end. The 1,191 and 1,050-bp-long DNA fragments carrying *lacUV5*(UP^{full}) have the start site positioned 706 and 602 bp from the downstream end, respectively. The 1,050-bp-long DNA fragment carrying *lacUV5*(UP^{prox}) has the start site positioned 602 bp from the downstream end. Details about the preparation of DNA fragments and proteins are provided in the supplementary information online.

Complex formation and AFM imaging. RP_o complexes were prepared by mixing 20 nM DNA with 20 nM RNAP in transcription buffer (20 mM Tris–HCl pH 7.9, 50 mM KCl, 5 mM $MgCl_2$). The 10 μl reaction was incubated at 37 °C for 15 min. The reaction was diluted to 1–2 nM complexes in 20 μl of deposition buffer (4 mM HEPES pH 7.4, 10 mM NaCl, 4 mM $MgCl_2$) and deposited onto freshly cleaved mica. The sample was incubated for about 2 min before the surface was rinsed with water and dried with nitrogen. AFM imaging was carried out in air with the tapping mode using a Nanoscope III microscope (Veeco Digital Instruments, Santa Barbara, CA, USA).

Supplementary information is available at *EMBO reports* online (http://www.emboreports.org).

ACKNOWLEDGEMENTS

We thank M. Thomas for plasmids and Centro Interfacoltà Misure for the AFM facility. This work was supported by the Italian Ministry of University and Scientific and Technological Research grant FIRB-RBNE01KMT9 to C.R. and by National Institutes of Health grant GM41376 and a Howard Hughes Medical Institute investigatorship to R.H.E.

REFERENCES

Aiyar SE, Gourse RL, Ross W (1998) Upstream A-tracts increase bacterial promoter activity through interactions with the RNA polymerase α subunit. *Proc Natl Acad Sci USA* **95:** 14652–14657

Blatter EE, Ross W, Tang H, Gourse RL, Ebright RH (1994) Domain organization of RNA polymerase α subunit: C-terminal 85 amino acids constitute a domain capable of dimerization and DNA binding. *Cell* **78:** 889–896

Busby S, Ebright RH (1994) Promoter structure, promoter recognition, and transcription activation in prokaryotes. *Cell* **79:** 743–746

Bustamante C, Rivetti C (1996) Visualizing protein–nucleic acid interactions on a large scale with the scanning force microscope. *Annu Rev Biophys Biomol Struct* **25:** 395–429

Bustamante C, Keller D, Yang G (1993) Scanning force microscopy of nucleic acids and nucleoprotein assemblies. *Curr Opin Struct Biol* **3:** 363–372

Coulombe B, Burton ZF (1999) DNA bending and wrapping around RNA polymerase: a 'revolutionary' model describing transcriptional mechanisms. *Microbiol Mol Biol Rev* **63:** 457–478

Davis CA, Capp MW, Record Jr MT, Saecker RM (2005) The effects of upstream DNA on open complex formation by *Escherichia coli* RNA polymerase. *Proc Natl Acad Sci USA* **102:** 285–290

Estrem ST, Gaal T, Ross W, Gourse RL (1998) Identification of an UP element consensus sequence for bacterial promoters. *Proc Natl Acad Sci USA* **95:** 9761–9766

Estrem ST, Ross W, Gaal T, Chen ZW, Niu W, Ebright RH, Gourse RL (1999) Bacterial promoter architecture: subsite structure of UP elements and interactions with the carboxy-terminal domain of the RNA polymerase α subunit. *Genes Dev* **13:** 2134–2147

Gourse RL, Ross W, Gaal T (2000) UPs and downs in bacterial transcription initiation: the role of the α subunit of RNA polymerase in promoter recognition. *Mol Microbiol* **37:** 687–695

Heddle JG, Mitelheiser S, Maxwell A, Thomson NH (2004) Nucleotide binding to DNA gyrase causes loss of DNA wrap. *J Mol Biol* **337:** 597–610

Koo HS, Wu HM, Crothers DM (1986) DNA bending at adenine · thymine tracts. *Nature* **320:** 501–506

Meng W, Savery NJ, Busby SJ, Thomas MS (2000) The *Escherichia coli* RNA polymerase α subunit linker: length requirements for transcription activation at CRP-dependent promoters. *EMBO J* **19:** 1555–1566

Naryshkin N, Revyakin A, Kim Y, Mekler V, Ebright RH (2000) Structural organization of the RNA polymerase–promoter open complex. *Cell* **101:** 601–611

Rippe K, Guthold M, von Hippel PH, Bustamante C (1997) Transcriptional activation via DNA-looping: visualization of intermediates in the activation pathway of *E. coli* RNA polymerase-s54 holoenzyme by scanning force microscopy. *J Mol Biol* **270:** 125–138

Rivetti C, Codeluppi S (2001) Accurate length determination of DNA molecules visualized by atomic force microscopy: evidence for a partial B- to A-form transition on mica. *Ultramicroscopy* **87:** 55–66

Rivetti C, Guthold M, Bustamante C (1996) Scanning force microscopy of DNA deposited on mica: equilibration versus kinetic trapping studied by polymer chain analysis. *J Mol Biol* **264:** 919–932

Rivetti C, Guthold M, Bustamante C (1999) Wrapping of DNA around the *E. coli* RNA polymerase open promoter complex. *EMBO J* **18:** 4464–4475

Ross W, Gourse RL (2005) Sequence-independent upstream DNA-αCTD interactions strongly stimulate *Escherichia coli* RNA polymerase–lacUV5 promoter association. *Proc Natl Acad Sci USA* **102:** 291–296

Ross W, Gosink KK, Salomon J, Igarashi K, Zou C, Ishihama A, Severinov K, Gourse RL (1993) A third recognition element in bacterial promoters: DNA binding by the α subunit of RNA polymerase. *Science* **262:** 1407–1413

Ross W, Aiyar SE, Salomon J, Gourse RL (1998) *Escherichia coli* promoters with UP elements of different strengths: modular structure of bacterial promoters. *J Bacteriol* **180:** 5375–5383

Verhoeven EE, Wyman C, Moolenaar GF, Hoeijmakers JH, Goosen N (2001) Architecture of nucleotide excision repair complexes: DNA is wrapped by UvrB before and after damage recognition. *EMBO J* **20:** 601–611

Zhang G, Campbell EA, Minakhin L, Richter C, Severinov K, Darst SA (1999) Crystal structure of *Thermus aquaticus* core RNA polymerase at 3.3 Å resolution. *Cell* **98:** 811–824